ARKIV FÖR FYSIK Band 1 nr 21

Communicated 11 May 1949 by MANNE SIEGBAHN and ERIK HULTHÉN

The red and green bands of magnesium oxide

By ALBIN LAGERQVIST and ULLA UHLER

With 4 figures in the text

Abstract. The visible band-systems of MgO, especially the red system, have been the subject of a new investigation. The analyses show that the red and green systems have the same upper level. The red bands represent a $^1\Sigma^* - {}^1\Pi$, the green ones a $^1\Sigma^* - {}^1\Sigma$ transition. The vibrational constants are

	ω_e	$x_e\,\omega_e$
Σ^*	824.0_8 cm^{-1}	4.7_6 cm^{-1}
Π	664.4_4 »	3.9_1 »
Σ	785.0_6 »	5.1_8 »

The rotational analyses gave the following constants (for Σ^* the mean values are taken from our analyses of the red and green bands):

	B_v	D_v	r_e
Σ^*	$0.5822 - 0.0045\,(v + \frac{1}{2})$	$[1.14 + 0.025\,(v + \frac{1}{2})] \cdot 10^{-6}$	$1.737 \cdot 10^{-8}$ cm
Π	$0.5056 - 0.0046\,(v + \frac{1}{2})$	$[1.184 - 0.005\,(v + \frac{1}{2})] \cdot 10^{-6}$	1.864
Σ	$0.5743 - 0.0050\,(v + \frac{1}{2})$	$[1.22 + 0.02\,(v + \frac{1}{2})] \cdot 10^{-6}$	1.749

A short discussion of the correlations between molecular states in MgO and atomic states in Mg and O is given.

Introduction

Magnesium oxide has two band-systems in the visible part of the spectrum, one situated in the red, the other in the green region. In 1932, MAHANTI (1) made vibrational analyses of these two systems and in 1935 (2) a rotational analysis of the red bands. In the latter paper he stated that the red bands represent a $^1\Sigma - {}^1\Sigma$ transition and analysed rotationally the 0,1, 0,0, 1,0 and 2,0 bands. In 1943 (3), one of the present authors made rotational analyses of the green bands. The result of this investigation showed that the green bands correspond to a $^1\Sigma - {}^1\Sigma$ transition. Only the 0,0 and 1,1 bands were analysed. It was, therefore, impossible to verify the combination differences.

The vibrational constants derived for the upper states of the two systems show a remarkable agreement. The rotational constants determined for the upper levels of these systems showed, however, no agreement at all. For the upper state MAHANTI determined B_e to 0.7625, for the upper state of the green system our previous value of B_e was 0.5822. Considering the resemblance of the vibrational constants it seemed us peculiar that the rotational constants did not agree. Thus it seemed desirable to repeat the investigation of the red bands as we already have good plates of the green ones. Our plates of the red system show very distinctly the presence of a Q-branch in addition to the R and P-branches (see Figs. 1 and 2). It is odd that MAHANTI did not notice the Q-branch. In the 1,0 band and 2,0 band especially — both analysed by MAHANTI — the Q-branch is very marked. Our rotational analyses show that the red and and green bands have the same upper level.

From this it follows that MAHANTI's rotational analysis is wrong. In this paper we give the rotational analyses of the 2,0, 1,0, 0,0, 0,1 and 0,2 transitions of the red bands. We show that earlier analyses of the green 0,0 and 1,1 bands are correct but for the J-numbering of the P-branches after the turn at the heads. The P-branches are formed of about 20 P-lines. In the 0,0 band the first P-line resolved after the head is P (78) not P (79) and in the 1,1 band P (73) instead of P (74). These alterations influence very little the magnitude of the B-values, which, however, we have determined again with respect to the new numbering of the P-branches. We have also analysed the 2,2 band of the green system.

Finally, we have drawn the Morse potential curves and discuss the probable atomic states into which the molecular states dissociate.

The red system

1. Experiments

The spectrograms were taken in the first order with a Wood's 21 ft concave grating (165 000 lines in all). The dispersion in the actual region is about 1.2 Å/mm.

An arc burning in air between water-cooled magnesium electrodes was used as the source of light. The current was about 8 A from a 440 Volt D. C. output. Using vertical electrodes only a rather short exposure time (about one hour) was needed, but in the background we obtained a disturbing continuum. With photographing only the red flame surrounding the arc less continuum appeared. The best way to obtain this red flame was to arrange the electrodes almost horizontally so that the top of the arc was photographed. The exposure-time was about 10 hours. Owing to the weak intensity of the red bands very sensitive plates, Eastman Kodak 1 F, were used. Several magnesium rods must be used for a single exposure. Iron lines taken from HARRISON's (4) tables were used for comparison.

2. Description of the bands

Every band consists of three branches, one of them more intense than the others, which are of the same intensity. Thus it is evident that the strongest

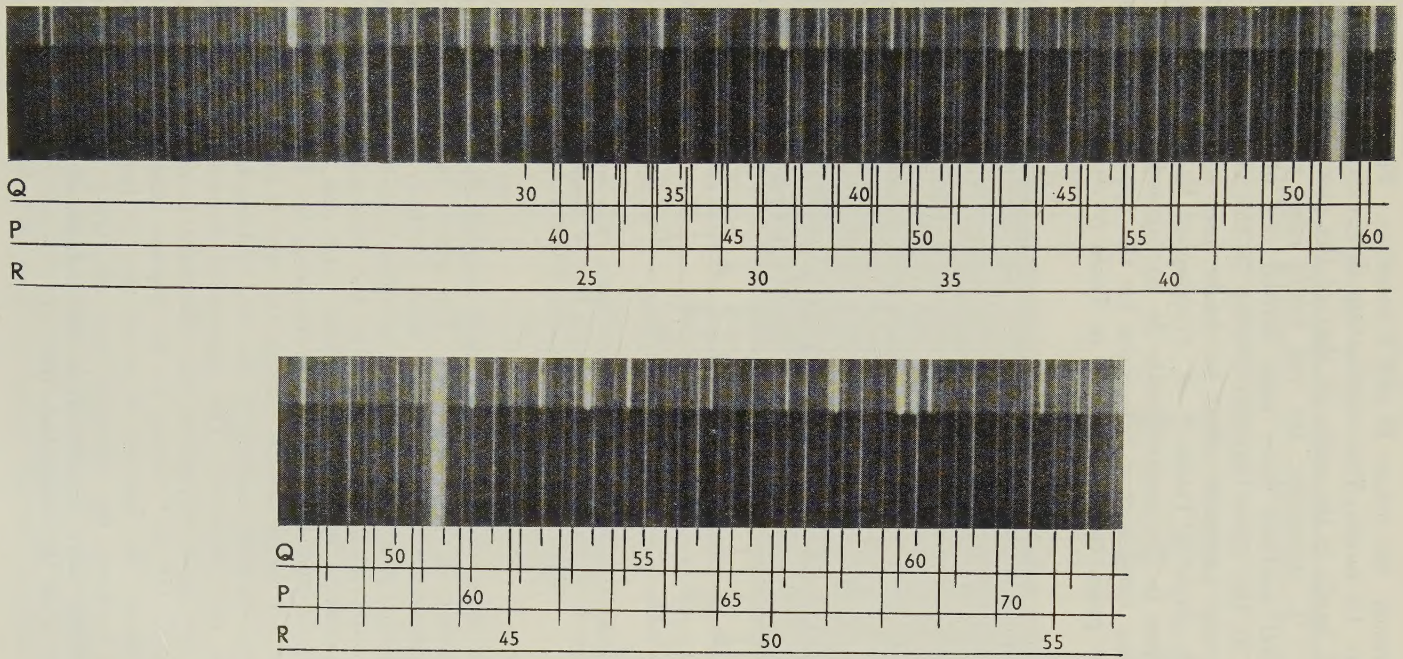

Fig. 1. The 1,0 band of the red system. The Q, P and R-branches are very marked. The reproductions show also the iron lines. The intense line at Q (51) is the magnesium line 5711.115 Å.

branch is a Q-branch, the others R and P-branches. Figs. 1 and 2 show the appearance of the 1,0 band. The combination differences show that the upper level of the red bands is the same as that of the green ones. As the latter represent a $^1\Sigma - {}^1\Sigma$ transition, the red bands must correspond to $^1\Sigma - {}^1\Pi$ system. Rotational analyses have been carried out of the 2,0, 1,0, 0,0, 0,1 and 0,2 bands. As the three branches overlap in the vicinity of the head, we have not made any particular effort to obtain lines with low J-values. The wave-numbers are given in Tables 1—5. Overlapped lines are marked with *. Generally the errors in the measurements do not exceed 0.04 cm^{-1}. The agreement between the combination differences for the upper Σ-state (determined from the red and green bands) is shown in Table 6.

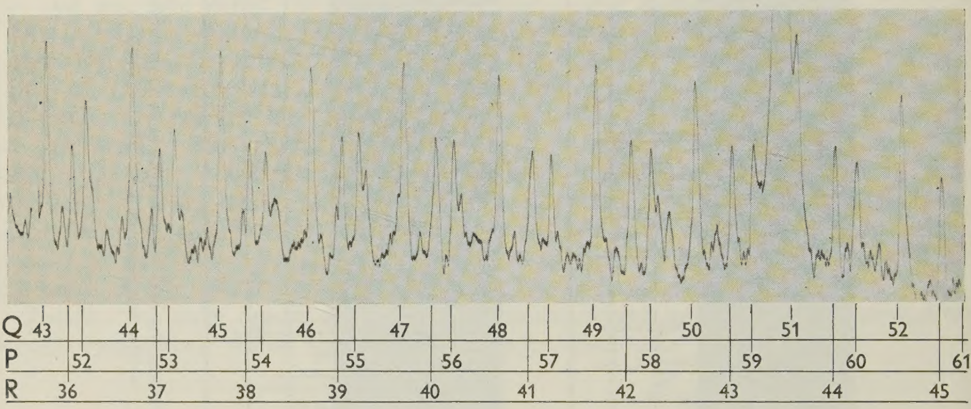

Fig. 2. Microphotograph showing a part of the 1,0 band. The intensity distribution of the Q, P and R-branches is of the ordinary type for a $\Pi - \Sigma$ transition. The intense line at Q (51) is the magnesium line 5711.115 Å.

Magnesium has three isotopes with atomic weights 24, 25 and 26 and with a relative abundance of about 7 : 1 : 1. The plates show several weak lines that might be referred to the isotopes. Some of them in the 1,0 band were measured and agreed very well with the calculated ones. As they are of little interest for the analysis, we have not given the isotopic lines here.

Regarding MAHANTI's wave-number tables, one can find that he has used alternately the Q, R and P-branches for obtaining his R and P-branches. For example, in the 1,0 band he has chosen the real Q-branch as his R-branch and his P-branch consists mainly of the real P-branch. The real R-branch, however, he has not observed. The agreement between our and his wave-numbers is not so good, sometimes the difference is negligible, sometimes it is of the magnitude 1.0 cm^{-1}, unless he has chosen other lines.

MAHANTI published the isotopic lines of the 0,0 band. The agreement is very good here between the observed and calculated values. MAHANTI has, however, only taken into consideration the rotational isotopic effect. The vibrational effect is of the magnitude 0.6 cm^{-1}.

Table 1

Structure of the 2,0 band

J	Q (J) cm^{-1}	R (J) cm^{-1}	P (J) cm^{-1}
19	18 145.53		
20	48.32*		
21	51.03		
22	54.03		
23	57.20		
24	60.39	18 188.79	
25	63.83	93.21	
26	67.26	97.91	
27	70.86	202.61	
28	74.65	07.55	
29	78.52	12.55	
30	82.58	17.68	18 148.32*
31	86.72	23.00	51.36
32	91.03	28.42	54.44
33	95.48	34.03	57.87
34	200.09	39.74	61.24
35	04.73	45.47	64.87
36	09.59	51.49	68.62
37	14.57	57.51	72.49
38	19.68	63.78	76.41
39	24.92	70.13	80.65
40	30.31	76.60	84.90
41	35.83	83.27	89.24
42	41.44	90.12	93.81
43	47.23	97.00	98.43
44	53.14	303.88	203.26
45	59.22	10.95	08.11
46	65.37	18.37	13.20
47	71.72	25.72	18.40
48	78.11	33.31	23.75
49	84.69	41.05	29.20
50	91.45	48.93	34.80
51	98.37	56.83	40.53
52	305.39	64.90	46.43
53	18 312.56	18 373.11	18 252.47
54	19.74	81.51	58.61
55	27.06	89.94	64.83
56	34.60	98.58	71.30
57	42.28	407.27	77.86
58	50.07	16.17	84.58
59	58.03	25.25	91.45
60	66.12	34.40	98.37
61	74.40		305.39
62	82.70	53.03	12.66
63	91.19	62.53	20.04
64	99.77	72.25	27.64
65	408.50	82.00	35.20
66	17.41	91.99	42.96
67	26.42	502.02	50.85
68	35.54	12.33	58.95
69	44.81	22.68	67.11
70	54.22	33.05	75.46
71	63.79	43.60	83.93
72	73.43	54.37	92.54
73	83.24	65.24	401.18
74		76.23	10.25
75	503.31	87.34	19.19
76	13.51	98.59	28.23
77	23.92	609.95	37.51
78	34.34	21.48	46.98
79	44.95	33.11	56.46
80	55.76	44.91	66.12
81	66.68	56.82	76.01
82	77.64	68.81	85.86
83	88.84	80.92	95.95
84	600.10	93.16	506.13
85	11.13	705.73	16.53
86	23.13		27.00
87	34.73	30.95	37.51
88	46.66	43.72	48.34
89	58.59	56.63	59.16
90	70.72		70.24
91	83.00		81.34
92	95.35		92.50
93	707.87		603.84
94	20.49		15.22
95	33.34		26.63
96	46.22		38.10
97	59.36		

Analysis

To get the rotational band-constants B_v and D_v we used the graphical method, plotting $\Delta_2 F(J)$ against $(J + \frac{1}{2})^2$, and obtained $4 B_v$ as the intersection with the ordinate, and $8 D_v$ from the inclination of the lines.

Table 2

Structure of the 1,0 band

J	Q (J) cm^{-1}	R (J) cm^{-1}	P (J) cm^{-1}	J	Q (J) cm^{-1}	R (J) cm^{-1}	P (J) cm^{-1}
8	17 320.23			56	17 544.96	17 609.39	17 481.09
9	21.39			57	53.20	18.75	88.21
10	22.75			58	61.56	28.24	95.49
11	24.42			59	70.08	37.83	502.88
12	26.07			60	78.76	47.54	10.37
13	28.06			61	87.51	57.39	18.07
14	29.96			62	96.48	67.44	25.92
15	32.13			63	605.57	77.57	33.85
16	34.51			64	14.77	87.89	42.04
17	36.91			65	24.16	98.37	50.26
18	39.53			66	33.67	708.92	58.67
19	42.27			67	43.34	19.71	67.23
20	45.12			68	53.19	30.52	75.97
21	48.15			69	63.11	41.61	84.83
22	51.32			70	73.20	52.73	93.84
23	54.64		17 328.06	71	83.43	63.99	602.94
24	57.95*	17 386.82	30.54	72	93.82	75.46	12.19
25	61.66*	91.46	32.87	73	704.34	87.06	21.65
26	65.46*	96.35	35.56	74	15.01	98.75	31.19
27	69.39*	401.36	38.30	75	25.83	810.64	40.91
28	73.38	06.58	41.15	76	36.83	22.66	50.80
29	77.59	11.86	44.23	77	47.93	34.79	60.80
30	81.93	17.32	47.23	78	59.15	47.05	70.96
31	86.38	22.92	50.74	79	70.57	59.56	81.26
32	90.97	28.66	54.17	80	82.08	72.13	91.76
33	95.72	34.55	57.95*	81	93.81	84.84	702.29
34	400.62	40.48	61.66*	82	805.64	97.59	13.06
35	05.68	46.73	65.46*	83	17.59	910.60	23.92
36	10.85	53.11	69.39*	84	29.76	23.76	34.92
37	16.20	59.57	73.81	85	41.98	37.01	46.15
38	21.64	66.18	78.13	86	54.39	50.37	57.41
39	27.28	72.96	82.60	87	66.93		68.85
40	33.05	79.85	87.22	88	79.59		80.42
41	38.99	86.84	92.09	89	92.46		92.19
42	45.00	94.03	96.94	90	905.43		804.04
43	51.25	501.34	402.01	91	18.54		16.02
44	57.60	08.81	07.20	92	31.84		28.16
45	64.10	16.43	12.63	93	45.28		40.36
46	70.73	24.18	18.05	94	59.23		52.67
47	77.51	32.03	23.70	95			65.08
48	84.49	40.05	29.49	96			77.41
49	91.49	48.23	35.39				
50	98.72	56.54	41.47				
51	506.04	64.99	47.74				
52	13.56	73.59	54.16				
53	21.22	82.39	60.64				
54	28.95	91.24	67.37				
55	36.90	600.30	74.17				

Table 3

Structure of the 0,0 band

J	Q (J) cm^{-1}	R (J) cm^{-1}	P (J) cm^{-1}	J	Q (J) cm^{-1}	R (J) cm^{-1}	P (J) cm^{-1}
16	16 521.20	16 540.74*		54	16 728.83*	16 791.63	16 666.65*
17	23.84	44.54*		55	37.33*	801.23	73.97
18	26.61	48.45*		56	45.96*	10.95	81.42
19	29.50	52.60*		57	54.74*	20.84	89.14
20	32.61	56.74*		58	63.63*	30.83	96.98
21	35.81	61.15*		59	72.75*	41.04	704.95
22	39.24	65.69*		60	81.94	51.38	13.01
23	42.76	70.36*		61	91.31	61.75	21.26
24	46.43	75.19*		62	800.92	72.39	29.63
25	50.31	80.30*	16 521.25	63	10.56	83.17	38.24
26	54.32	85.49*	24.17	64	20.37	94.12	47.03
27	58.48	90.75*	27.20	65	30.43	905.18	55.92
28	62.73	96.26*	30.14	66	40.60	16.45	64.88
29	67.09		33.48	67	50.86	27.90	74.13
30	71.83	607.58*	37.08	68	61.33	39.49	83.51
31	76.59	13.51*	40.74*	69	71.94	51.16	92.96
32	81.52	19.58*	44.54*	70	82.75	62.95	802.65
33	86.61	25.85*	48.45*	71	93.63	75.08	12.52
34	91.85	32.20*	52.60*	72	904.70	87.22	22.45
35	97.23	38.76*	56.74*	73	15.95	99.50	32.62
36	602.75	45.36*	61.15*	74	27.36	17 011.90	42.88
37	08.47	52.15	65.69*	75	38.89	24.45	53.30
38	14.30	59.07	70.36*	76	50.63	37.25	63.89
39	20.26	66.27	75.19*	77	62.47		74.63
40	26.44	73.60	80.30*	78	74.56		85.61
41	32.75	81.08	85.49*	79	86.72	76.20	96.67
42	39.26	88.72	90.75*	80	99.02	89.57	907.73
43	45.86	96.46*	96.26*	81	17 011.52	103.20	19.16
44	52.57	704.32*		82	24.09	116.87	30.67
45	59.54	12.33*	607.58*	83	36.85		42.44
46	66.65*	20.53*	13.51*	84			54.27
47	73.88	28.83*	19.58*	85			66.04
48	81.25	37.33*	25.85*	86			78.37
49	88.75	45.96*	32.20*	87			90.56
50	96.46*	54.74*	38.76*	88			17 002.91
51	704.32*	63.63*	45.36*	89			15.63
52	12.33*	72.75*	52.24	90			28.69
53	20.53*	82.17	59.45	91			42.41

For the Λ-doubled Π-state the following combination differences were used

$$\Delta_2 F''_d (J) = R(J-1) - P(J+1)$$

and

$$\Delta_2 F''_c (J) = R(J) - P(J) - Q(J+1) + Q(J-1).$$

The graphical method gives the effective band-constants B_d and B_c. The real B-value is taken as the mean value of B_d and B_c. The constants derived are

Table 4

Structure of the 0,1 band

J	Q (J) cm^{-1}	R (J) cm^{-1}	P (J) cm^{-1}	J	Q (J) cm^{-1}	R (J) cm^{-1}	P (J) cm^{-1}
14		15 877.40		48	16 035.55	16 091.50	15 980.12
15	15 863.23	81.38*		49	43.54	100.63	86.92
16	65.90	85.50		50	51.67	09.87	93.89
17	68.64	89.45		51	59.97	19.33	16 001.07
18	71.50	93.50		52	68.49	28.88	08.37
19	74.68	97.84		53	77.11	38.63	15.93
20	77.98	902.22		54	85.91	48.56	23.63
21	81.38*	06.83		55	94.88	58.66	31.47
22	84.83	11.47		56	104.02	68.85	39.47
23	88.71	16.51		57	13.34	79.23	47.54
24	92.65	21.57		58	22.77	89.74	55.94
25	96.82*	26.73		59	32.44	200.43*	64.39
26	900.90	32.10		60	42.19	11.30*	73.07
27	05.36	37.63		61	52.15	22.32*	81.90
28	09.92	43.40		62	62.21		90.84
29	14.67	49.28		63	72.54		100.00
30	19.62	55.22		64	82.98		09.31
31	24.62	61.48		65	93.57		18.82
32	29.82	67.83		66	204.36		28.35
33	35.22	74.40		67	15.27		38.15
34	40.75	81.02	15 901.41	68	26.38		48.08
35	46.46	87.85	05.96	69			58.15
36	52.31	94.87	10.65	70			68.45
37	58.40	16 001.99	15.47	71			78.48
38	64.55	09.39	20.55	72			89.47
39	70.93	16.87	25.85	73			200.36*
40	77.45	24.54	31.12	74			11.30*
41	84.14	32.29	36.68	75			22.32*
42	91.01	40.26	42.39				
43	98.05	48.42	48.33				
44	16 005.17	56.75	54.33				
45	12.54	65.24	60.54				
46	20.03	73.74	66.85				
47	27.70	82.58	73.37				

$^1\Sigma^*$ state	$^1\Pi$ state
$B'_0 = 0.5799$ cm^{-1}	$B''_0 = 0.5033$ cm^{-1}
$B'_1 = 0.5754$	$B''_1 = 0.4987$
$B'_2 = 0.5708$	$B''_2 = 0.4941$
$D'_0 = 1.15 \cdot 10^{-6}$ cm^{-1}	$D''_0 = 1.18 \cdot 10^{-6}$ cm^{-1}
$D'_1 = 1.18$	$D''_1 = 1.18$
$D'_2 = 1.21$	$D''_2 = 1.17$

Table 5

Structure of the 0,2 band

J	Q (J) cm^{-1}	R (J) cm^{-1}	P (J) cm^{-1}	J	Q (J) cm^{-1}	R (J) cm^{-1}	P (J) cm^{-1}
13	15 210.40			46	15 381.10	15 434.63	15 327.71
14	12.87			47	89.16	43.86	34.65
15	15.55			48	97.47	53.31	41.73
16	18.33			49	405.87	62.70	49.01
17	21.22			50	14.47	72.39	56.46
18	24.27			51	23.25	82.29	64.09
19	27.53			52	32.18	92.32	71.89
20	31.00			53	41.34	502.57	79.92
21	34.61			54	50.62	12.97	88.04
22	38.44			55	60.10	23.52	96.36
23	42.36			56	69.75	34.19	404.81
24	46.43	15 275.37	15 218.63	57	79.53	45.07	13.40
25	50.80	80.75	21.78	58	89.53	56.15	22.31
26	55.50	86.46	25.09	59	99.74	67.29	31.25
27		92.21	28.63	60	510.06	78.65	40.38
28	64.80	98.19	32.21	61	20.57	90.29	49.75
29	69.75	304.28	36.09	62	31.27	601.95	59.19
30	74.95	10.59	40.13	63	42.11	13.85	68.89
31	80.25	17.06	44.29	64	53.15	25.85	78.66
32	85.77	23.70	48.60	65	64.32	38.02	88.67
33	91.49	30.46	53.13	66	75.64	50.40	98.77
34	97.32	37.52	57.80	67	87.20	62.84	509.06
35	303.37	44.61	62.73	68	98.94		19.61
36	09.52	51.98	67.74	69	610.81		30.22
37	15.92	59.46	72.97	70	22.92		40.99
38	22.45	67.15	78.42	71	35.11		51.86
39	29.15	75.03	83.95	72	47.49		62.86
40	36.08	83.17	89.65	73	60.02		73.99
41	43.12	91.22	95.49	74	72.74		85.19
42	50.40	99.59	301.65	75	85.74		96.46
43	57.78	408.00	07.90	76	98.91		607.77
44	65.37	16.72	14.35	77	712.00		18.96
45	73.09	25.63	20.92	78			29.95

The band-constants can be combined in the equations

$$B'_v = 0.5822 - 0.00455\,(v + \tfrac{1}{2});\ \ B''_v = 0.5056 - 0.0046\,(v + \tfrac{1}{2})$$

$$D'_v = [1.135 + 0.03\,(v + \tfrac{1}{2})] \cdot 10^{-6};\ \ D''_v = [1.184 - 0.005\,(v + \tfrac{1}{2})] \cdot 10^{-6}.$$

The internuclear distances are

$$r'_e = 1.737 \cdot 10^{-8}\ \text{cm} \qquad r''_e = 1.864 \cdot 10^{-8}\ \text{cm}.$$

According to KRATZER's relation, the calculated D_e-values are:

$$D'_e = 1.16 \cdot 10^{-6}\ \text{cm}^{-1} \qquad D''_e = 1.17 \cdot 10^{-6}.$$

Table 6

The combination differences $\Delta_2 F'(J)$ of the Σ^*-state

J	v′ = 0				v′ = 1		v′ = 2	
	The red 0,2 band	The red 0,1 band	The red 0,0 band	The green 0,0 band	The red 1,0 band	The green 1,1 band	The red 2,0 band	The green 2,2 band
24	56.74			56.66	56.28	56.33		55.81
25	58.97		59.05	59.12	58.59	58.55		58.08
26	61.37		61.25	61.26	60.79	60.79		60.35
27	63.58		63.52	63.63	63.06	63.11		62.63
28	65.98		66.08	65.91	65.43	65.37		64.96
29	68.19		68.32	68.20	67.63	67.58		67.07
30	70.46		70.50	70.45	70.09	70.04	69.36	69.34
31	72.77		72.77	72.79	72.21	72.19	71.64	71.65
32	75.10		75.04	75.04	74.49	74.50	73.98	73.99
33	77.33		77.40	77.35	76.60	76.77	76.16	76.07
34	79.72	79.61	79.60	79.67	78.82	79.00	78.50	78.33
35	81.88	81.89	82.02	81.96	81.27	81.25	80.60	80.64
36	84.24	84.22	84.21	84.17	83.72	83.65	82.87	82.88
37	86.49	86.52	86.46	86.54	85.76	85.87	85.02	85.16
38	88.73	88.84	88.71	88.80	88.05	88.12	87.37	87.30
39	91.08	91.02	91.08	91.07	90.36	90.41	89.48	89.61
40	93.52	93.42	93.30	93.34	92.63	92.67	91.70	91.87
41	95.73	95.61	95.51	95.57	94.75	94.94	94.03	94.07
42	97.94	97.87	98.03	97.83	97.09	97.05	96.31	96.29
43	100.10	100.09	100.24	100.11	99.33	99.36	98.57	98.55
44	102.37	102.42	102.52	102.38	101.61	101.57	100.62	100.73
45	104.71	104.70	104.75	104.68	103.80	103.83	102.84	102.96
46	106.92	106.89	107.02	106.91	106.13	106.06	105.17	105.16
47	109.21	109.21	109.25	109.17	108.33	108.28	107.32	
48	111.58	111.38	111.48	111.49	110.56	110.55	109.56	
49	113.69	113.71	113.76	113.76	112.84	112.80	111.85	
50	115.93	115.98	115.98	115.97	115.07	115.06	114.13	
51	118.20	118.26	118.27	118.28	117.25	117.26	116.30	
52	120.43	120.51	120.51	120.42	119.43	119.48	118.47	
53	122.65	122.70	122.68	122.75	121.75	121.77	120.64	
54	124.93	124.93	124.98		123.87		122.90	
55	127.16	127.19	127.30		126.13		125.11	
56	129.38	129.38	129.55		128.30		127.28	
57	131.67	131.69	131.70		130.54		129.41	
58	133.84	133.90	133.85		132.75		131.59	
59	136.04	135.97	136.09		134.95		133.80	
60	138.27	138.23	138.37		137.17		136.03	
61	140.54	140.42	140.49		139.32			
62	142.76		142.76		141.52		140.37	
63	144.96		144.93		143.72		142.49	
64	147.19		147.09		145.85		144.61	
65	149.35		149.23		148.11		146.80	
66	151.63		151.57		150.25		149.03	
67	153.78		153.77		152.48		151.17	
68			155.98		154.55		153.38	
69			158.20		156.78		155.45	
70			160.30		158.89		157.59	157.46
71			162.56		161.05		159.67	159.62
72			164.77		163.27		161.83	161.76

Table 6 (cont.).

J	$v' = 0$				$v' = 1$		$v' = 2$	
	The red 0,2 band	The red 0,1 band	The red 0,0 band	The green 0,0 band	The red 1,0 band	The green 1,1 band	The red 2,0 band	The green 2,2 band
73			166.88		165.41	165.45	163.93	163.97
74			169.02		167.56	167.59	165.98	166.01
75			171.15		169.73	169.74	168.15	168.10
76			173.42		171.86	171.92	170.36	170.27
77					173.99	174.07	172.44	172.36
78				177.59	176.09	176.23	174.50	174.63
79			179.53	179.69	178.30	178.20	176.65	176.80
80			181.84	181.86	180.37	180.34	178.79	178.78
81			184.04	183.98	182.55	182.39	180.81	181.00
82			186.20	186.16	184.53	184.46	182.95	182.96
83				188.30	186.68	186.63	184.97	185.10
84				190.46	188.84	188.76	187.03	187.10
85				192.52	190.86	190.91	189.20	189.31
86				194.64	192.96	192.95		191.39
87				196.72		195.09	193.44	193.44
88				198.87		197.21	195.38	195.50
89				200.96		199.24	197.47	197.55
90				203.20		201.30		199.55

Λ-type doubling

The sum of the Λ-type doubling of two adjacent rotational levels in the Π-state is equal to the combination defect $\varepsilon(J)$

$$\varepsilon(J) = R(J) - Q(J) - Q(J+1) + P(J+1).$$

The expression for $\varepsilon(J)$ is

$$\varepsilon(J) = 2\,(B^d_v - B^c_v)\,J\,(J+1).$$

Plotting $\varepsilon(J)$ against $J(J+1)$, we determined $B^d_v - B^c_v$ from the inclinations of the lines obtained. The results are

$$B^d_0 - B^c_0 = 0.0001$$

$$B^d_1 - B^c_1 = 0.0001$$

$$B^d_2 - B^c_2 = 0.0002.$$

The green bands

Description of the bands

The green bands represent a ${}^1\Sigma - {}^1\Sigma$ transition. It is characteristic of the band-lines that they are considerably closer together than the red ones. The bands form a very narrow Condon parabola, and for this reason it was

Table 7

Structure of the 2,2 band

J	R (J) cm^{-1}	P (J) cm^{-1}	J	R (J) cm^{-1}	P (J) cm^{-1}
14	20 103.13	20 070.06	53	20 171.46	
15	04.43*	69.17	54	73.53	
16	05.88*	68.32	55	75.77	
17	07.41	67.44	56	77.91	
18	08.88	66.64*	57	80.10	
19	10.37*	65.94*	58	82.31	
20	11.87*	65.16*	59	84.43	
21	13.39	64.36	60	86.82	
22	14.93	63.60	61	88.95	
23	16.48	62.93	62	91.30	
24	18.02	62.21	63	93.55	
25	19.65*	61.57*	64	95.91	
26	21.25	60.90*	65	98.21	
27	22.85	60.22*	66	200.41*	
28	24.48	59.52*	67	02.98*	
29	26.02	58.95	68	05.28	
30	27.79*	58.45	69	07.75*	
31	29.53	57.88	70	10.18	20 052.72*
32	31.27	57.28	71	12.67	53.05*
33	32.95	56.88	72	15.13	53.37*
34	34.69	56.36*	73	17.61	53.64*
35	36.49	55.85*	74	20.13	54.12*
36	38.23*	55.35*	75	22.64*	54.54*
37	40.06	54.90*	76	25.17	54.90*
38	41.84	54.54*	77	27.71	55.35*
39	43.73	54.12*	78	30.48	55.85*
40	45.61	53.74*	79	33.16	56.36*
41	47.44	53.37*	80	35.81	57.03*
42	49.34	53.05*	81	38.54	57.54
43	51.27	52.72*	82	41.24	58.28*
44	53.21	52.48	83	43.90	58.80*
45	55.14	52.18	84	46.72	59.62
46	57.10	51.94*	85	49.53	60.22*
47	59.09		86	52.29	60.90*
48	61.11		87	55.01	61.57*
49	63.12		88	57.90	62.40
50	65.16*		89	60.83	63.28
51	67.14		90	63.71	64.16
52	69.32		91	66.63	64.92

previously impossible to check the combination differences as only the 0,0 and 1,1 bands could be analysed (LAGERQVIST (3)). As the agreement between the combination differences of the upper levels of the red and green bands is very good, it is of no interest to analyse the very weak and hardly accessible 0,1 and 1,0 bands. On the other hand, we have analysed the 2,2 band. The wave-numbers of this band are given in Table 7. A comparison between the combination differences of the upper levels of the red and green bands appears in Table 6.

Analysis

In our previous paper on the green bands, rotational band-constants were given. These have here been re-calculated by the graphical method and with regard to the alteration in J-numbering of the P-branches. With the combination differences obtained from the red bands we were able to show that after the turn at the head the J-numbering of the P-lines ought to be altered by one unit. Thus in the 0,0 band the first P-line resolved after the head is P (78) not P (79), and in the 1,1 band P (73) not P (74). The constants obtained are

$B'_0 = 0.5799\ \mathrm{cm}^{-1}$ $\qquad B''_0 = 0.5718\ \mathrm{cm}^{-1}$

$B'_1 = 0.5754$ $\qquad B''_1 = 0.5668$

$B'_2 = 0.5709$ $\qquad B''_2 = 0.5618$

$D'_0 = 1.16 \cdot 10^{-6}\ \mathrm{cm}^{-1}$ $\qquad D''_0 = 1.23 \cdot 10^{-6}\ \mathrm{cm}^{-1}$

$D'_1 = 1.17$ $\qquad D''_1 = 1.25$

$D'_2 = 1.20$ $\qquad D''_2 = 1.27$

The band-constants can be combined in the equations

$$B' = 0.58215 - 0.0045\,(v + \tfrac{1}{2});\ \ B'' = 0.5743 - 0.0050\,(v + \tfrac{1}{2})$$

$$D' = [1.15 + 0.02\,(v + \tfrac{1}{2})]\,10^{-6};\ \ D'' = [1.22 + 0.02\,(v + \tfrac{1}{2})] \cdot 10^{-6}$$

The internuclear distance $r''_e = 1.749 \cdot 10^{-8}$ cm

The agreement between the band-constants for the upper Σ-level calculated from the red and green bands is very good.

According to KRATZER's relation the D''_e-value is

$$D''_e = 1.23 \cdot 10^{-6}\ \mathrm{cm}^{-1}.$$

Vibrational constants and some discussions on MgO

Vibrational constants

The band-origins for the red bands have been calculated from the Q-branches as the positions of Q (0) (G. HERZBERG (5)). For the green bands they are determined from the equation

$$R\,(J - 1) + P\,(J) = 2\,\nu_0 + 2\,(B' - B'')\,J^2$$

The result is

ν_0 for the red bands		ν_0 for the green bands	
2,0	$18\,119.8_9$	0,0	$20\,003.5_7$
1,0	$17\,314.8_5$	1,1	$20\,043.4_3$
0,0	$16\,500.2_9$	2,2	$20\,084.1_3$
0,1	$15\,843.6_7$		
0,2	$15\,194.8_7$		

From the positions of the band-origins, we got the following values for the vibrational constants

	Σ^*	Π	Σ
ω_e	824.0_8	664.4_4	785.0_6
$x_e \omega_e$	4.7_6	3.9_1	5.1_8

Dissociation energies and potential curves

It is difficult to give reliable values for the dissociation energies as we know only the three lowest vibrational states. The dissociation energies were determined from the approximate formula

$$D_e = \frac{\omega_e^2}{4\, x_e\, \omega_e}.$$

The values obtained are

$$D_e(\Sigma^*) = 35\,700 \text{ cm}^{-1} \quad (4.40 \text{ e.v.})$$
$$D_e(\Pi) = 28\,200 \quad (3.48 \text{ e.v.})$$
$$D_e(\Sigma) = 29\,800 \quad (3.68 \text{ e.v.})$$

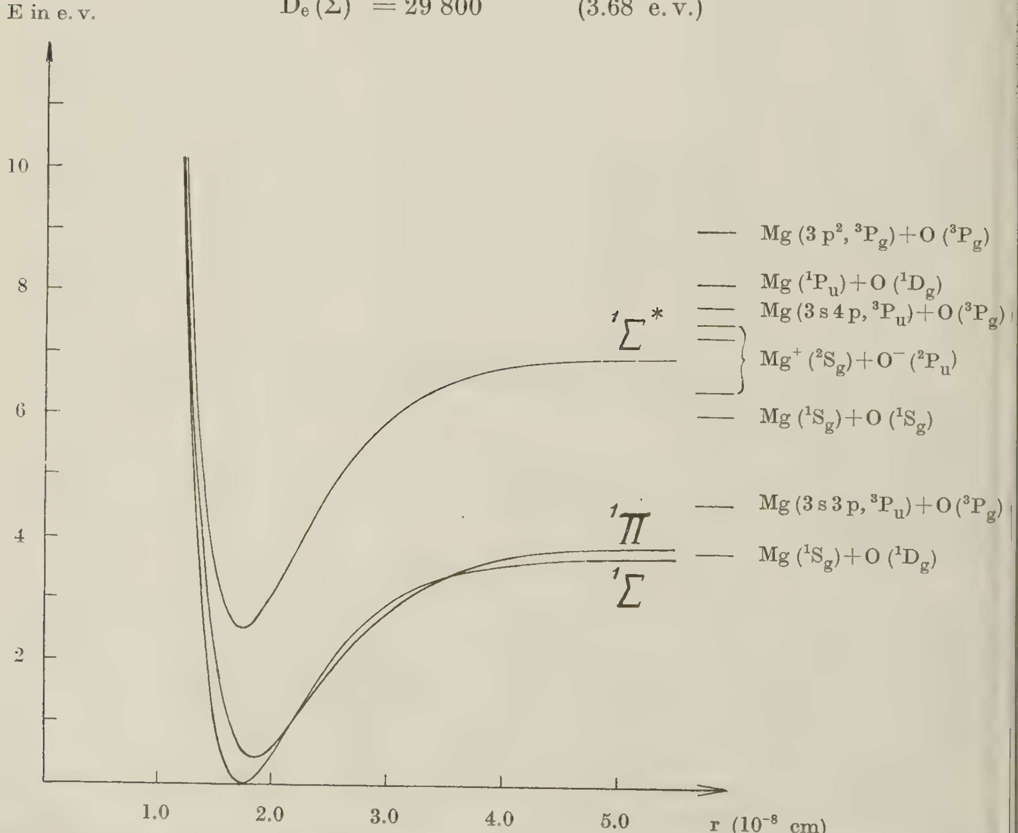

Fig. 3. Potential curves of the known states in MgO and the states of the separate atoms.

The Morse curves have been drawn (Fig. 3), using these values for the dissociation energies and the other band-constants. The upper Σ-state is everywhere denoted by Σ^*.

Correlations between molecular and atomic states

In order to discuss the correlations between the molecular and atomic states it is necessary to know whether the Σ-states of MgO are Σ^+ or Σ^--states. Placing all the electrons in the lowest possible orbitals, we obtain, using MULLIKEN's notations, the following configuration (KKL) $(z\,\sigma)^2\,(y\,\sigma)^2\,(w\,\pi)^4$, which gives a $^1\Sigma^+$-state. Alternating the electron configuration it is very difficult to find any combination giving birth to a $^1\Sigma^-$-state. Both the known $^1\Sigma$-states must therefore be $^1\Sigma^+$-states. We assume that the lowest Σ-state is the normal state with the electron configuration mentioned above.

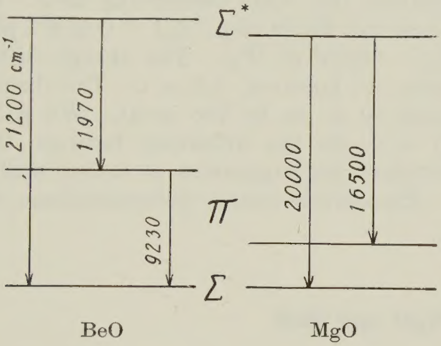

Fig. 4. The electronic levels and transitions in BeO and MgO.

As our knowledge of the dissociation energies is very uncertain, it is a delicate matter to discuss the correlations between the molecular and atomic states and we will therefore stress that our suggestions are only tentative.

We will underline the resemblance between the spectra of BeO and MgO. BeO like MgO has three electronic states Σ^*, Π and Σ, situated in the same way (Fig. 4). Thus it is probable, that the molecular states of BeO and MgO dissociate into the same atomic states of the metal and oxygen. A detailed discussion of BeO is given by one of us (6).

From Fig. 3 we see that the difference between the dissociation limits are: $\Sigma \to \Sigma^*$ 3.2 e.v., $\Pi \to \Sigma^*$ 3.0 e.v. The lowest atom pair giving a $^1\Sigma^+$-state is Mg (^1S_g) + O (^3P_g). This combination also corresponds to a $^1\Pi$-state. From the relative positions of the potential curves for Σ and Π we presume that Σ and Π dissociate into the same atom pair, namely Mg (^1S_g) + O (^3P_g). In Fig. 3 we have placed these atomic terms opposite to the dissociation limits of Σ and Π. Above these atomic terms we have drawn other possible atomic constellations leading to $^1\Sigma^+$-states. The first possibility for getting a $^1\Sigma^+$-state, apart from Mg (^3P_u) + O (^3P_g), is Mg (^1S_g) + O (^1S_g). The difference between this atom pair and Mg (^1S) + O (^1D) is 2.2 e. v. This does not agree very well with that for $\Sigma \rightarrow \Sigma^*$, 3.2 e. v., but considering the uncertainty of the dissociation energies, Mg (^1S) + O (^1S) may, nevertheless, be the dissociation limit for Σ^*. Another alternative is that Σ^* dissociates into $Mg^+ + O^-$. This suggestion might also explain the deep minimum in the potential curve for Σ^*. Our knowlegde of the electron affinity is, however, poor. LOZIER (7) and HANSON (8) obtained 51 ± 5 Kcal and 46 ± 9 Kcal/mol respectively, using electron methods. VIER and MAYER (9), on the contrary, made new determinations some years ago and got the surprising result 70.8 ± 0.8 Kcal. Thus the energy difference between $Mg^+ + O^-$ and Mg (^1D) + O (^1D) lies between the limits 2.6 e. v. and 3.7 e. v. In any case, it is not out of the question that Σ^* dissociates into $Mg^+ + O^-$.

MAHANTI (10) is of the same opinion concerning MgO as G. HERZBERG (11) and LESSHEIM and SAMUEL (12) were concerning BeO. He suggests that the normal state corresponds to Mg (3 s 3 p, ^3P_u) + O (2 s^2 2 p^4, ^3P_g) and the upper Σ-state to Mg (3 p^2, ^3P_g) + O (2 s^2 p^4, ^3P_g). The energy difference between these two atom configurations is, however, 4.5 e. v. The discrepancy between this value and 3.2 e. v. seems to us to be too great. We will add, however, that MAHANTI obtained 4.1 e. v. for the difference between the dissociation limits for Σ^* and Σ, and therefore his suggestion is rather well-grounded. Owing to the uncertainty of the dissociation energy determinations, this possibility should be bourne in mind.

Comparison between MgO and BeO

As has already been mentioned the spectra of MgO and BeO are very similar. Fig. 4 shows the well-known electronic states of these molecules. The green system $\Sigma^* - \Sigma$ of MgO corresponds to the blue $\Sigma^* - \Sigma$ bands of BeO, and the red MgO bands to the weak infra-red inter-combination system $\Sigma^* - \Sigma$ of BeO. That no bands corresponding to the strong $\Pi - \Sigma$ infra-red BeO bands are found in MgO depends on the fact that these MgO bands are situated so far out in the infra-red region, beyond the sensitivity of the photographic plates.

In the rotational levels of the electronic states Σ^* and Π of BeO a lot of perturbations are found (6). Several of the Σ^*-levels were perturbed by Π-levels and several Π-levels by Σ-levels. We should of course also expect such perturbations in the MgO bands. No such interactions are, however, found. An extrapolation of the energies for Σ and Π-levels shows that rotational perturbations ought to be situated at about $J = 75$ and $J = 90$ in the vibrational levels $v = 3$ and 2 of Π, respectively, and for the levels $v = 1$ and 0 at still higher J-values. In the Π-state we have only analysed the levels $v = 0,1$ and 2, and have not been able to follow the branches to lines with such high J-numbers. This fact explains why no perturbations are found in the Π-state. One would expect that the upper Σ^*-state ought to be perturbed by levels from the Π-state. We have, however, not noticed any perturbations in the Σ^*-state. They must, therefore, be too small to be detected in the vibrational Σ^*-levels investigated.

In the ultra-violet region there are a lot of complicated bands in the spectrum of MgO as in that of BeO. The analysis of these MgO bands seems to be as difficult as that of the BeO bands.

Physics Department, The University, Stockholm, May 1949.

REFERENCES. 1. **Mahanti, P. C.**, Phys. Rev. *42*, 609, 1932. — 2. ——, Ind. Journ. Phys. *9*, 455, 1935. — 3. **Lagerqvist, A.**, Ark. f. Mat., Astr. o. Fys. *29 A*, No. 25, 1943. — 4. **Harrison, G. R.**, Wavelength Tables, New York, 1939. — 5. **Herzberg, G.**, Molekülspektren und Molekülstruktur, Dresden und Leipzig, 1939. — 6. **Lagerqvist, A.**, Inaugural Dissertation, Uppsala, 1948. — 7. **Lozier, W.**, Phys. Rev. *46*, 268, 1934. — 8. **Hanson, G.**, Phys. Rev. *48*, 476, 1935. — 9. **Vier, D. T.** and **Mayer, J. E.**, J. Chem. Phys. *12*, 28, 1944. — 10. **Mahanti, P. C.**, Ind. Journ. Phys. *9*, 517, 1935. — 11. **Herzberg, G.**, ZS. f. Phys. *57*, 601, 1929. — 12. **Lessheim, H.** and **Samuel, R.**, ZS. f. Phys. *84*, 637, 1933.

Tryckt den 4 november 1949

Uppsala 1949. Almqvist & Wiksells Boktryckeri AB